AL-ZAHRAA UNIVERSITY JOURNAL
Health and Medical Science

*Al-Zahraa Journal for Health and Medical Sciences 2026; 4(1):*215-242 **Vol. 4, No.1, 2026**
www.zjhms.alzahraa.edu.iq

Tri-substituted Imidazole complexes: Synthesis, Characterization and Biological Evaluation

Elaf Q. Abdulkadum[1*] , Jihan Hameed Abdulameer[1]

[1]Department of Chemistry, College of Education for Pure Sciences, University of Kerbala. Karbala, Iraq
* ielaf.q@s.uokerbala.edu.iq

Received: 14 March (2026), Accepted: 28 March 2026. Published: 31 March 2026

ABSTRACT

This study explores the design and synthesis of novel tri-imidazole derivatives and their corresponding metal chloride complexes. The tri-imidazole ligand was synthesized via a multi-component condensation reaction involving benzil, ammonium acetate, and salicylaldehyde derivatives. Coordination of this ligand with platinum(IV), palladium(II), nickel(II), and copper(II) chloride salts yielded a series of stable solid-state metal complexes. The structural architectures of the synthesized compounds were elucidated using a comprehensive suite of spectroscopic and analytical techniques, including UV–Visible, FT-IR, and ^{1}H-NMR spectroscopy, alongside mass spectrometry, elemental analysis, magnetic susceptibility, and molar conductivity measurements. Metal content was precisely determined via Atomic Absorption Spectroscopy (AAS). Spectroscopic evidence confirmed that the ligand coordinates as a bidentate chelating agent. Geometric analysis revealed that the [L–Pt] complex adopts an octahedral configuration, whereas the [L–Pd], [L–Ni], and [L–Cu] complexes exhibit square planar geometries. The biological efficacy of the synthesized compounds was evaluated against selected microbial strains and cancer cell lines to assess their antibacterial, antifungal, and cytotoxic potential. The results demonstrated that the metal complexes possess significantly enhanced bioactivity compared to the free ligand. Notably, the platinum complex [L–Pt] exhibited superior biological performance, outperforming all other synthesized complexes. Furthermore, when compared to the clinical gold standard, Cisplatin, the [L–Pt] complex demonstrated higher potency, establishing it as the most effective antibacterial and anticancer agent in this study. These findings highlight the [L–Pt] complex as a promising candidate for the development of advanced Metallo therapeutic drugs.

AL ZAHRAA UNIVERSITY JOURNAL
Health and Medical Science

*Al-Zahraa Journal for Health and Medical Sciences 2026; 4(1):*215-242 **Vol. 4, No.1, 2026**
www.zjhms.alzahraa.edu.iq

Keywords: Tri-imidazole derivatives, Bidentate chelating agent, Anticancer & Antibacterial activity, Structure-Activity Relationship (SAR), Metal-based drugs (Metallodrugs).

Introduction

Metal complexes containing ligands with biologically active heteroatoms—particularly oxygen (O), nitrogen (N), and sulfur (S)—have attracted considerable scientific attention in recent years. This growing interest is largely attributed to their enhanced biocidal properties, including bactericidal, fungicidal, herbicidal, and insecticidal activities, as well as their expanding applications in clinical pharmacology [1]. Among these ligands, imidazole represents a significant class of heterocyclic compounds. Imidazole is a five-membered aromatic ring composed of three carbon atoms and two nitrogen atoms. It constitutes a key structural motif in numerous biologically important molecules, including the amino acid histidine, vitamin B_{12}, DNA, and biotin [2]. Owing to its unique electronic structure and coordination ability, imidazole and its derivatives display a wide range of pharmacological activities, such as antimicrobial, anti-inflammatory, antitumor, and antidepressant effects, thereby occupying a central role in contemporary medicinal chemistry [3].In addition, amides form another essential functional group widely encountered in both natural and synthetic systems[4]. The remarkable stability of the amide bond makes it indispensable in organic synthesis, agrochemical formulations, and pharmaceutical development[5,6]. Furthermore, the electron-donating characteristics of the oxygen and nitrogen atoms in amide groups enable effective coordination with metal ions, facilitating the formation of stable metal complexes and thereby enhancing their biological and chemical applications[7]. This study aims to investigate and compare the antimicrobial and anticancer activities of a series of synthesized Nickel(II), Copper(II), Palladium(II), and Platinum(IV) complexes. These complexes feature a bidentate ligand derived from imidazole derivatives, synthesized to evaluate the influence of the metal center on their biological potency.

2. Experimental

2.1. Tools and Materials

All solvents and chemical reagents employed in this investigation, including $K_2PtCl_6 \cdot 6H_2O$ (analytical grade) supplied by Merck (Schnelldorf, Germany), $CoCl_2 \cdot 6H_2O$ and $NiCl_2 \cdot 6H_2O$,

IRAQI Academic Scientific Journals

AL ZAHRAA UNIVERSITY JOURNAL
Health and Medical Science

*Al-Zahraa Journal for Health and Medical Sciences 2026; 4(1):*215-242 **Vol. 4, No.1, 2026**
www.zjhms.alzahraa.edu.iq

$CuSO_4 \cdot 5H_2O$ (BDH), and $PdCl_2$ (Merck), were used as received without any additional purification. The melting points of the synthesized compounds were measured using a Stuart melting point apparatus. Structural elucidation of the prepared complexes was achieved through spectroscopic techniques. Electronic absorption spectra were recorded on a Shimadzu UV-1601 UV–Visible spectrophotometer employing quartz cuvettes, with absolute ethanol serving as the reference (baseline) solvent. Furthermore, Fourier Transform Infrared (FT-IR) spectra of the free ligands and their corresponding metal complexes were obtained using a Shimadzu FT-IR 8300 spectrophotometer over the wavenumber range of 4000–200 cm^{-1}, ^{1}H-NMR spectra were recorded on a [NMR Bruker 500mhz] , 400 MHz spectrometer using DMSO-d^6 as a solvent and TMS as an internal standard, Mass spectra were obtained using an Agilent 5973 mass spectrometer via the direct injection technique, Molar conductivity of 1×10^{-3} M solutions in ethanol was measured using a [Digital Conductivity Meter - WT - 720 – ino Lab, Germany] conductivity meter, Magnetic susceptibility measurements were performed at room temperature using a [Balance of Johnson mattey catalytic system divisionn at 25 ^{o}C] balance.

2.2. Experiments

2.2.1. Synthesis of tri-substituted imidazole ligand

In a 100 mL round-bottom flask, 0.2703 g of benzil, 0.175 g of the selected aldehyde (cinnamaldehyde), and 0.3854 g of ammonium acetate (as a nitrogen source essential for ring closure) were introduced. Glacial acetic acid (15 mL) was added as both solvent and catalyst. The reaction mixture was heated under reflux at 100–120 °C with continuous stirring for 6–12 hours until completion of the reaction. A noticeable color change was observed during the course of the reaction. Upon completion, the reaction mixture was allowed to cool to room temperature and then slowly poured into 100 mL of ice-cold distilled water to induce precipitation of the product. A few drops of aqueous ammonia were added to enhance precipitate formation. The resulting solid was collected by filtration, thoroughly washed several times with deionized water to remove any residual base and inorganic salts, and then dried to afford the pure imidazole derivative.

IRAQI Academic Scientific Journals

AL ZAHRAA UNIVERSITY JOURNAL
Health and Medical Science

*Al-Zahraa Journal for Health and Medical Sciences 2026; 4(1):*215-242 **Vol. 4, No.1, 2026**
www.zjhms.alzahraa.edu.iq

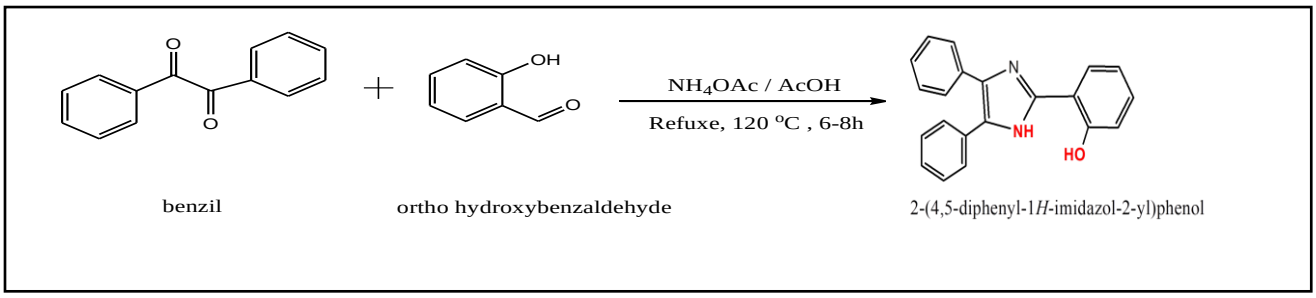

Scheme 1. Synthesis of the Ligand

2.2.2. Synthesis of complexes

The solid metal complexes were synthesized via a direct coordination reaction between the synthesized tri-imidazole ligand and the respective metal chloride salts. In a typical procedure, a solution of the tri-imidazole ligand (2.0 mmol) was prepared by dissolving it in a minimum amount of hot absolute ethanol. To this solution, a stoichiometric amount (1.0 mmol) of the corresponding metal ions : nickel (II), copper (II), palladium (II) and platinum (IV), dissolved in the same solvent was added dropwise under continuous magnetic stirring. In a 50 mL round-bottom flask, 0.156 g of the ligand (L) was dissolved in 5 mL of ethanol with continuous stirring. A solution of nickel (II) chloride hexahydrate (0.12 g) in 10 mL of ethanol was added dropwise to the ligand solution. The reaction mixture was refluxed at 60–65 °C for 3 hours. Upon completion, the formed precipitate was isolated by filtration and dried. The copper(II), palladium(II) and platinum(IV), and complexes were synthesized following the same experimental protocol, using 0.044 g of palladium(II) chloride, 0.122g of potassium hexachloro platinate(IV), and 0.0623 g of Copper(II) sulfate pentahydrate, respectively.

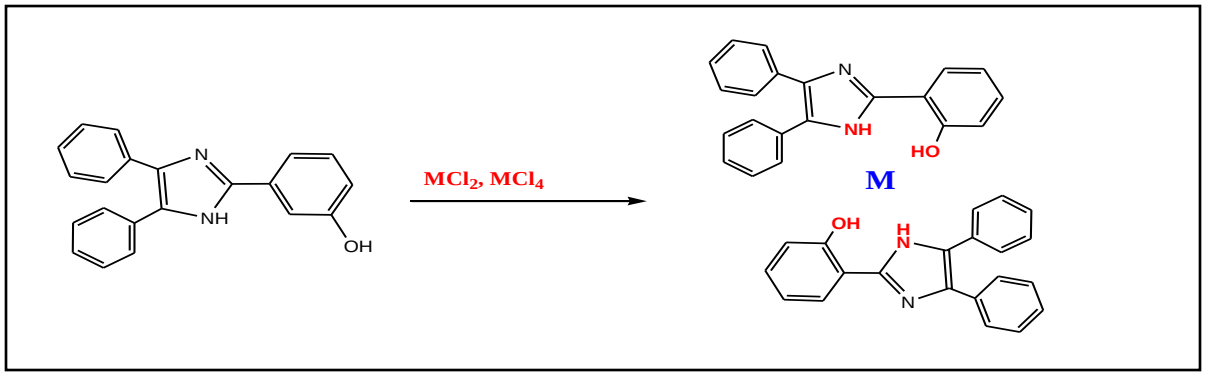

Scheme 2. Synthesis of the Complexes

IRAQI Academic Scientific Journals

AL ZAHRAA UNIVERSITY JOURNAL
Health and Medical Science

*Al-Zahraa Journal for Health and Medical Sciences 2026; 4(1):*215-242 **Vol. 4, No.1, 2026**
www.zjhms.alzahraa.edu.iq

2.3. Determination method of antimicrobial activity

The Kirby-Bauer assay was employed to assess the antimicrobial activity of tetra-imidazole ligand (L) and the newly synthesized complexes against the fungal pathogen *Candida albicans* and two bacterial strains: one Gram-negative (*Pseudomonas aeruginosa*) and one Gram-positive (*Streptococcus pneumoniae*) [8]. Twenty-four-hour-old bacterial cultures were previously inoculated onto nutrient-rich agar plates to evaluate antibacterial activity. Test compounds were applied to sterile Whatman No. 3 filter paper discs (6 mm diameter) and allowed to dry under a laminar flow biosafety cabinet. The discs were then aseptically and evenly placed onto the inoculated agar surfaces [9]. To standardize diffusion and reduce variability arising from differences in application timing, all bacterial- and fungal-inoculated plates were pre-chilled at 4 °C for one hour [10]. The plates were subsequently incubated at 37 °C for 24 hours, after which clear zones of inhibition surrounding the discs were observed [11-12], indicating antimicrobial activity[13]. The diameters of the inhibition zones were measured and recorded in millimeters for quantitative analysis [14].

2.4. Determination of Cytotoxicity Using MDA-MB-231 Cells

MDA-MB-231 breast cancer cells were obtained from the Biotechnology Research Center, Al-Nahrain University, and were used to determine the cytotoxic effects of the test compounds. Cells were treated with varying concentrations of all ligands and complexes (400, 200, 100, 50, 25, and 12.5 µg/mL). Untreated MDA-MB-231 cells were included as negative controls, along with additional untreated control cells, to ensure baseline measurements [15]. Furthermore, Cisplatin was utilized as a positive reference drug to benchmark the cytotoxicity of the tested complexes.

3. Results and Discussion

As shown in Table 1, the synthesized metal complexes exhibited distinct colors, while the ligand (L) employed in this study appeared yellow. The complexes were obtained in good yields, ranging from 60% to 86%, and demonstrated stability upon exposure to light and air. The metal complexes were characterized using a variety of analytical techniques, including UV–Vis

IRAQI Academic Scientific Journals

AL ZAHRAA UNIVERSITY JOURNAL
Health and Medical Science

*Al-Zahraa Journal for Health and Medical Sciences 2026; 4(1):*215-242 **Vol. 4, No.1, 2026**
www.zjhms.alzahraa.edu.iq

spectroscopy, Fourier-transform infrared (FT-IR) spectroscopy, ^{1}H NMR spectroscopy, magnetic moment determination, atomic absorption (A.A.) analysis, elemental analysis (C.H.N) and molar conductivity measurements. The experimental findings were in good agreement with the analytical data. Additionally, the measured magnetic susceptibility values of the synthesized complexes supported the proposed molecular geometries.

Table 1. The summary of the physicochemical properties of the ligand (L) and their corresponding metal complexes.

Com.	Color	Molecular weight g/mole	M.p.(°C)	Yield(%)	C.H.N analysis Found(calc)			%Metal Found(calc)	Molecular formula
					C	H	N		
L	White	312.37	198-203	60	80.32 (80.75)	5.03 (5.16)	8.21 (8.97)	-------	$C_{21}H_{16}N_2O$
L-Ni	Light red	752.31	120-123	68	66.85 (67.05)	4.00 (4.02)	7.11 (7.45)	7.25 (7.80)	$C_{42}H_{30}N_4NiO_2$
L-Cu	Purple	757.17	143-145	75	66.07 (66.62)	3.48 (3.99)	7.19 (7.40)	8.20 (8.39)	$C_{42}H_{30}CuN_4O_2$
L-Pd	Light brown	800.04	170-173	80	62.77 (63.05)	3.15 (3.78)	6.80 (7.00)	13.16 (13.30)	$C_{42}H_{30}N_4O_2Pd$
L-Pt	Yellow	888.7	163-165	86	56.39 (56.76)	3.10 (3.40)	6.12 (6.30)	21.55 (21.95)	$C_{42}H_{30}Cl_2N_4O_2Pt$

3.1 FT-IR Spectra of the Ligand (L) and Complexes

In the solid state, the FT-IR spectra of the ligand (L) and its prepared metal complexes were recorded, and the corresponding data are presented in Table (2). The measurements were carried out using the KBr and CsI pellet technique over the spectral range of 4000–400 cm^{-1} and 4000-200 cm^{-1} respectively. Infrared spectroscopy was utilized to identify the functional groups present in the free ligand and to monitor any changes in the characteristic absorption bands resulting from coordination with transition metal ions and the subsequent formation of metal complexes. In addition, comparing the obtained spectral results with previously reported literature values assists in identifying the probable coordination sites of the metal ion within the ligand framework [16]. The FT-IR spectrum of the tri-imidazole ligand (L) exhibits characteristic absorption bands corresponding to its functional groups, providing valuable insight into its potential coordination behavior. The broad band observed at 3203 cm^{-1} is attributed to the N–H stretching vibration of the imidazole ring, and its broadness is likely due to hydrogen

IRAQI Academic Scientific Journals

AL ZAHRAA UNIVERSITY JOURNAL
Health and Medical Science

*Al-Zahraa Journal for Health and Medical Sciences 2026; 4(1):*215-242 **Vol. 4, No.1, 2026**
www.zjhms.alzahraa.edu.iq

bonding interactions. The absorption band at 3069 cm^{-1} corresponds to the aromatic (sp^2) C–H stretching vibrations of the imidazole rings [17]. The band appearing at 1672 cm^{-1} is assigned to the C=N stretching vibration within the aromatic imidazole ring. Additionally, the bands at 1597 and 1550 cm^{-1} are attributed to C=C and C=N vibrational modes of the aromatic ring system. The absorption band at 1457 cm^{-1} is associated with C–H bending vibrations within the ring. The region between 1284 and 1018 cm^{-1} is assigned to C–N stretching vibrations of the imidazole framework [18]. While the FT-IR spectra of Ni(II), Cu(II), Pd(II) and Pt(IV) complexes with the tri-substituted imidazole ligand exhibited a symmetric coordination pattern, indicating a similar mode of binding across all complexes. A significant shift was observed in the C=N stretching bands compared to the free ligand, appearing at1597–1664 cm^{-1} for Ni(II), 1602 cm^{-1} for the Cu(II) complex, 1595–1676 cm^{-1} for Pd(II) and 1672 cm^{-1} for Pt(IV), suggesting the involvement of the imidazole nitrogen in coordination. The C–N stretching bands in the 1400–1100 cm^{-1} region also showed slight shifts in position and intensity for all complexes, further supporting metal–ligand interactions. Moreover, new bands appeared in the low-frequency region (400–600 cm^{-1}), observed at (478,605) cm^{-1} for (Ni–N) and (Ni–O) , (503,603) cm^{-1} for (Cu–N) and (Cu-–O),(509,569) cm^{-1} for (Pd–N) and (Pd–O), (495-609) cm^{-1} for (Pt–N) and (Pt–O). These bands are attributed to ν(M–N) and (M–O) vibrations, confirming the formation of coordination bonds between the metal centers with oxygen and nitrogen atoms [19]. These spectroscopic observations are consistent with the presence of N–H bands, which indicate the tri-substituted nature of the ligand. The spectra demonstrate that the ligand behaves as a bidentate donor through the nitrogen and oxygen atoms in all four complexes, with characteristic N–H band shifts at 3373 cm^{-1} for Ni(II), 3169 cm^{-1} for Cu(II), 3437 cm^{-1} for Pd(II), 3390 cm^{-1} for Pt(IV). While the absence of the O–H band in the IR spectra confirms the involvement of the oxygen atom in complexation with the metal ions and the absorption band appearing at 312 cm^{-1} exhibits weak intensity and is assigned to the (Pt-Cl) coordinate bond stretching. Based on the spectroscopic data and the electronic configuration of the metal ions, a square planar geometry is proposed for the Pd(II), Cu(II), and Ni(II) complexes, whereas the Pt(IV) complex is likely to adopt a distorted octahedral geometry [20].

IRAQI Academic Scientific Journals

AL ZAHRAA UNIVERSITY JOURNAL
Health and Medical Science

*Al-Zahraa Journal for Health and Medical Sciences 2026; 4(1):*215-242 **Vol. 4, No.1, 2026**
www.zjhms.alzahraa.edu.iq

Table 2. Selected bands of FT-IR spectra of the ligand and complexes synthesis in (cm^{-1})

Com.	ν (N–H)	ν (O–H)	ν (C–N)	ν (C=N)	ν (M–O)	ν (M–N)
L	3203	3200-3000	1284-1018	1672	----	----
L–Ni	3373	----	1261-1361	1597–1664	569	478
L–Cu	3169	----	1260-1315	1602	603	503
L–Pd	3437	----	1249-12-92	1595–1676	569	509
L–Pt	3390	----	1159-1261	1672	609	495

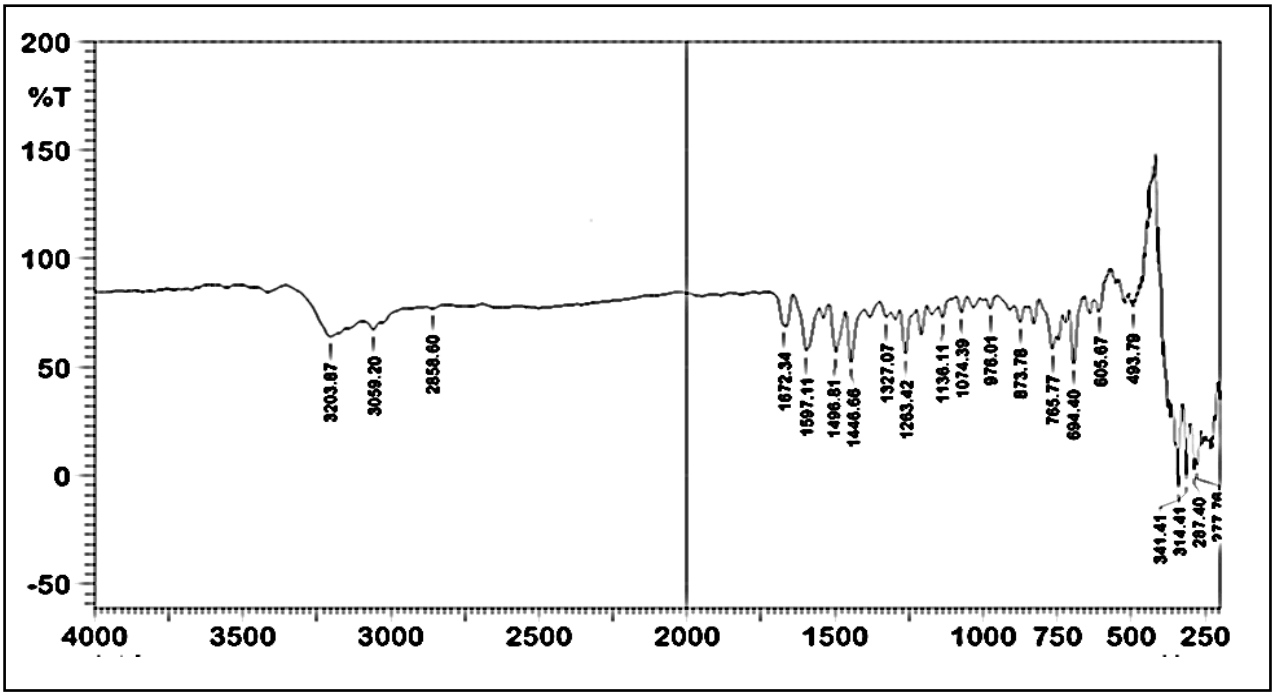

Fig. 1. FT.IR spectrum of the ligand(L).

IRAQI Academic Scientific Journals

AL ZAHRAA UNIVERSITY JOURNAL
Health and Medical Science

*Al-Zahraa Journal for Health and Medical Sciences 2026; 4(1):*215-242 **Vol. 4, No.1, 2026**
www.zjhms.alzahraa.edu.iq

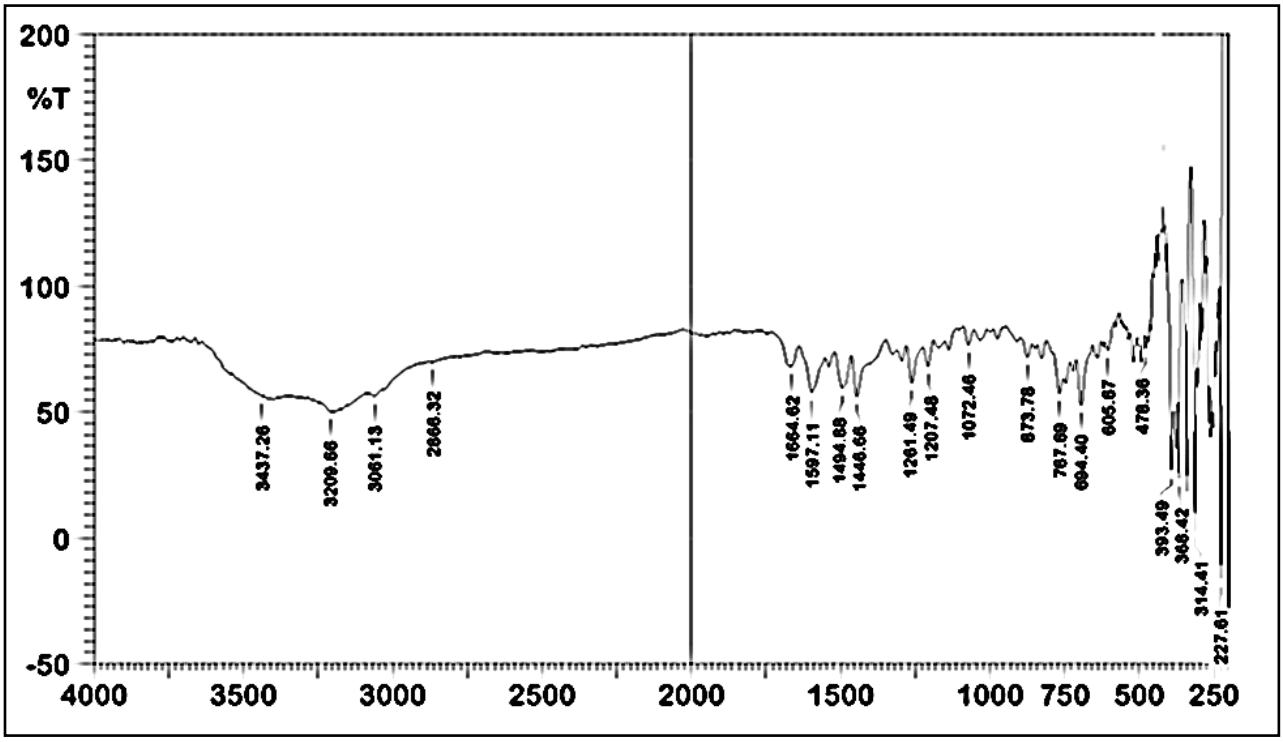

Fig. 2. FT.IR spectrum of the Ni(II)-L complex

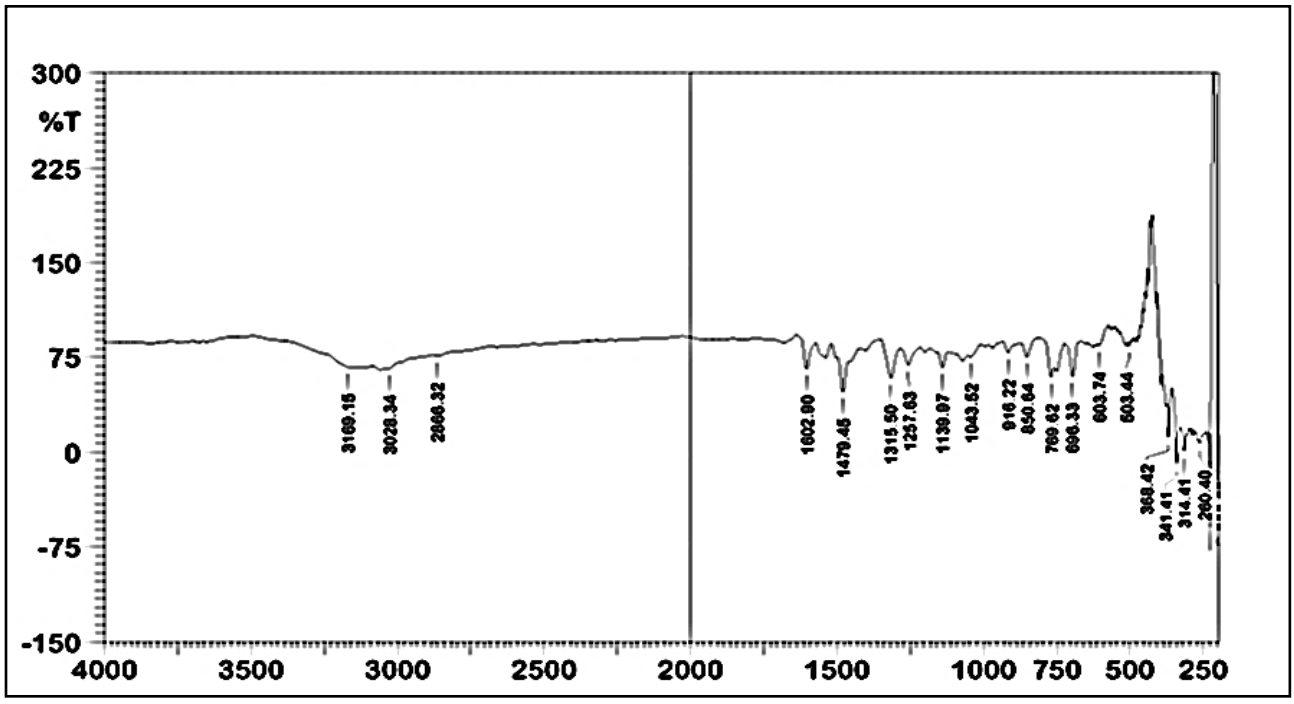

Fig. 3. FT.IR spectrum of the Cu(II)-L complex

IRAQI Academic Scientific Journals

AL ZAHRAA UNIVERSITY JOURNAL
Health and Medical Science

*Al-Zahraa Journal for Health and Medical Sciences 2026; 4(1):*215-242 **Vol. 4, No.1, 2026**
www.zjhms.alzahraa.edu.iq

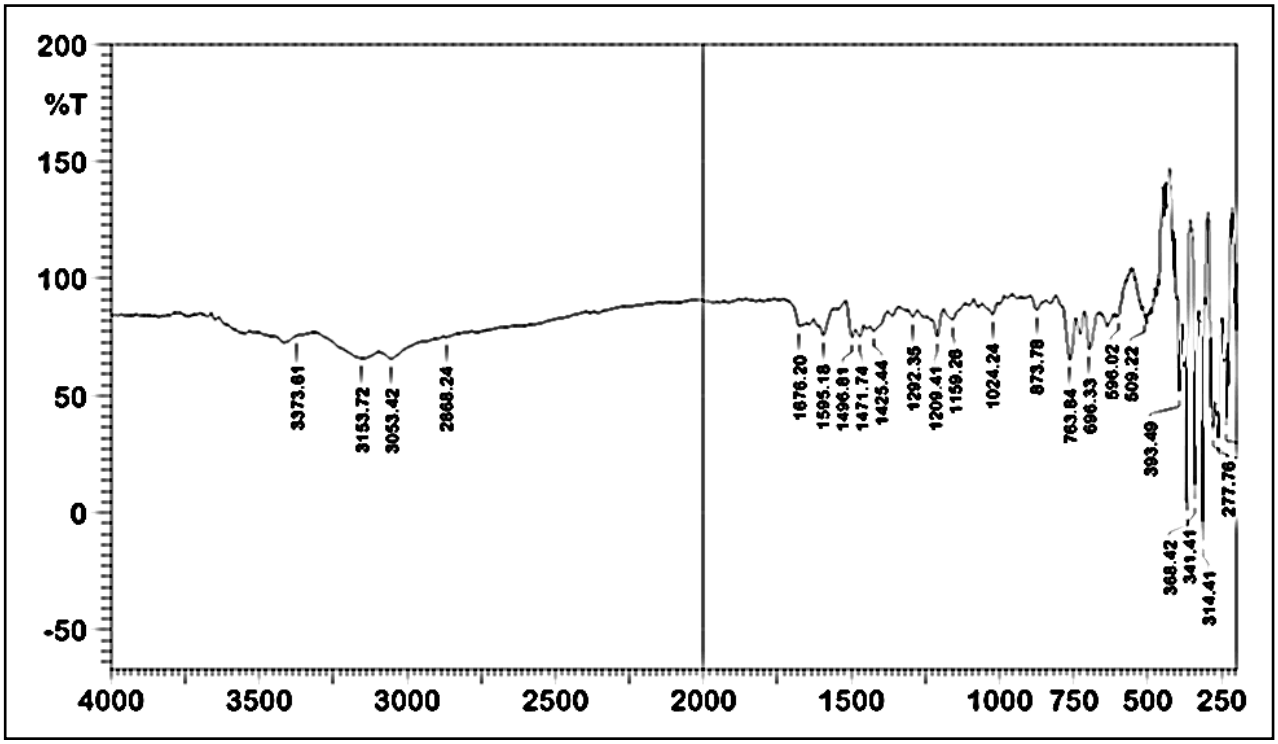

Fig. 4. FT.IR spectrum of the Pd(II)-L complex

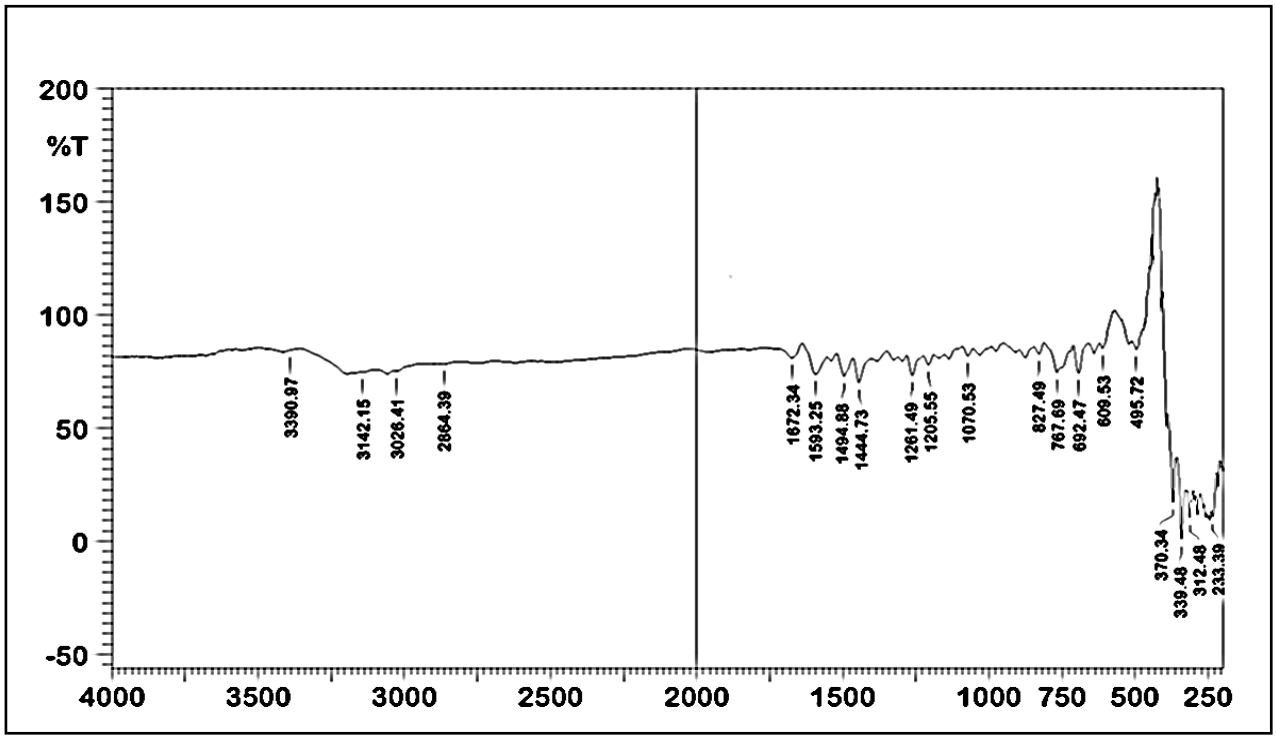

Fig. 5. FT.IR spectrum of the Pt(IV)-L complex

AL ZAHRAA UNIVERSITY JOURNAL
Health and Medical Science

*Al-Zahraa Journal for Health and Medical Sciences 2026; 4(1):*215-242 **Vol. 4, No.1, 2026**
www.zjhms.alzahraa.edu.iq

3.2. Electronic spectra, Magnetic susceptibility and Conductivity measurements: -

The UV-Vis spectra of ligand (L) are shown in Figure (6). The electronic spectra of (L) showed the two basic bands, the first of which was band that first appeared at 45330 cm-1 as a result of an inter ligand transition (π→π*) that took place on the π-system. The second band, located at 41234 cm-1, is also produced by the (n→π*) transition in another group [14], The Light red Ni(II) complex spectrum. The electronic spectra of this complex are depicted in Figure (7), with two main bands at 23825 and 35744 cm-1, corresponding to the 1A1g→1B1g and 1A1g→1Eg transitions, and another peak appearing at 44060 cm-1, which is attributed to charge transfer in a square planar geometry [21] and zero magnetic moment. This chemical appears to have a nonelectrolyte based on its conductivity behavior. The Purple Cu(II) complex spectrum. The electronic spectra of this complex are depicted in Figure (8), with two main bands at 28322 and 35653 cm-1, corresponding to the 1A1g→1B1g and 1A1g→1Eg transitions, which is attributed to charge transfer in a square planar geometry [22] and 1.81 B.M magnetic moment. This chemical appears to have a nonelectrolyte based on its conductivity behavior. The Brown Pd(II) complex's UV-Vis spectrum shows two bands. As seen in Figure (9), the two absorption bands occurred at 42000 cm^{-1} and the first absorption band at 33120 cm-1. The transition 1A1g → 1B1g, represented by 10Dq, has been assigned to these absorption bands, the transition 1A1g →1Eg Which represents the second absorption for spin- parried d8 square planar configuration [23]. The magnetic moment of the crystalline complex was found to be (Zero B.M.). The conductance behavior suggests that this compound has a nonelectrolyte. Figure (10) displays the electronic spectra of the produced Yellow Pt(IV) complex, with absorption bands corresponding to the transition at 26416 and 36910 cm-1. 1T2g → 1A1g, 1A1g →1T1g. The band that was observed at 9925 cm-1 is associated with spin-forbidden transitions. 1A1g → 3T1g, 3T2g. These, in accordance with accounts, suggested an octahedral geometry [24,25]. This result was related to t2g6eg0 configuration spin pair octahedral stereochemistry. The magnetic moment of the crystalline complex was found to be (Zero B.M.). The conductance behavior suggests that this compound has a nonelectrolyte. Moreover, the proposed square planar geometry for these Ni(II),Cu(II) and Pd(II) complexes was validated by data analysis and spectroscopy techniques[26]. However, this Pt(IV) complex was proposed to have an octahedral shape. as displayed in Table 3.

IRAQI Academic Scientific Journals

AL ZAHRAA UNIVERSITY JOURNAL
Health and Medical Science

*Al-Zahraa Journal for Health and Medical Sciences 2026; 4(1):*215-242 **Vol. 4, No.1, 2026**
www.zjhms.alzahraa.edu.iq

Table 3. Electronic spectra, Magnetic susceptibility and Conductivity measurements ligands complexes in (cm^{-1})

Com.	Abs:cm^{-1}	Assignment	μ eff B.M	μs .cm	Suggested geometry
L	45330 41234	π→π* n→π*	----	----	----
L–Ni	23825 35744	$^1A_1g \rightarrow {}^1B_1g$ $^1A_1g \rightarrow {}^1Eg$	0	19	square planar
L–Cu	28322 35653	$^1A_1g \rightarrow {}^1B_1g$ $^1A_1g \rightarrow {}^1Eg]'$	1.81	7	square planar
L–Pd	42000 33120	$^1A_1g \rightarrow {}^1B_1g$ $^1A_1g \rightarrow {}^1Eg$	0	14	square planar
L–Pt	26416 36910 9925	$^1T_2g \rightarrow {}^1A_1g$ $^1A_1g \rightarrow {}^1T_1g$ $^1A_1g \rightarrow {}^3T_1g, {}^3T_2g$	0	23	Octahedral

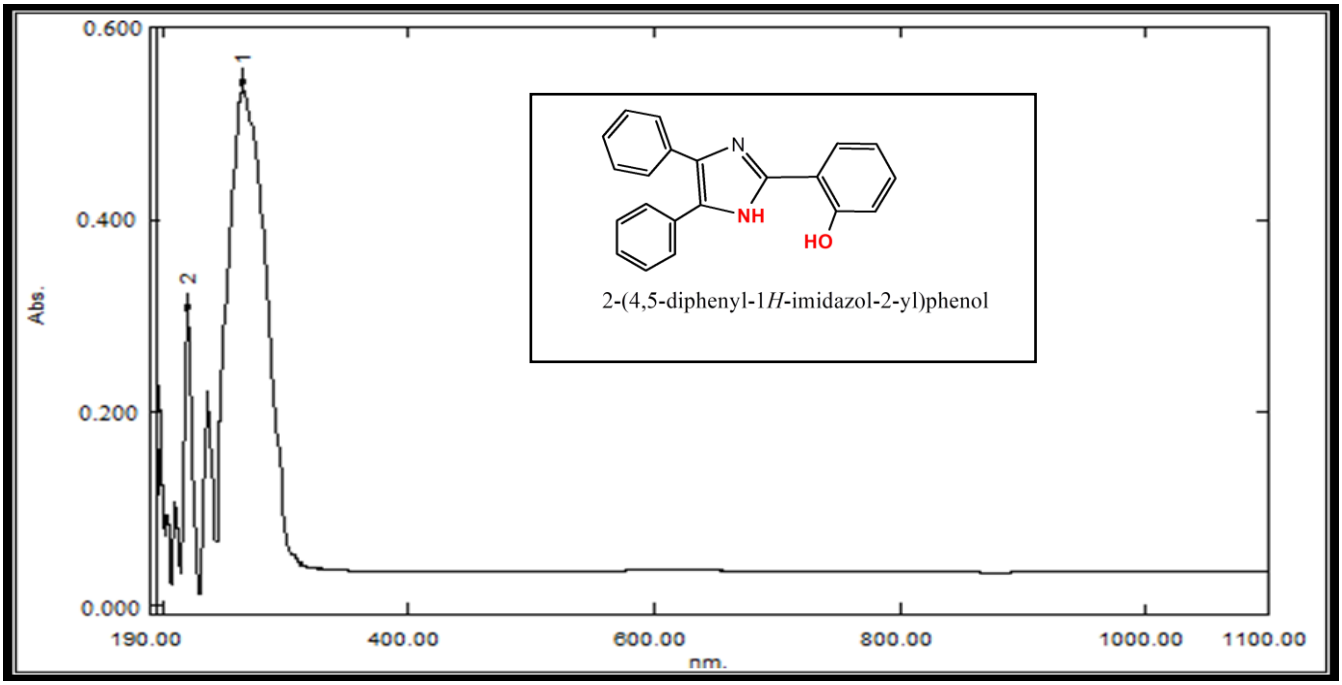

Fig. 6. Electronic spectrum of ligand(L)

IRAQI Academic Scientific Journals

AL ZAHRAA UNIVERSITY JOURNAL
Health and Medical Science

*Al-Zahraa Journal for Health and Medical Sciences 2026; 4(1):*215-242 **Vol. 4, No.1, 2026**
www.zjhms.alzahraa.edu.iq

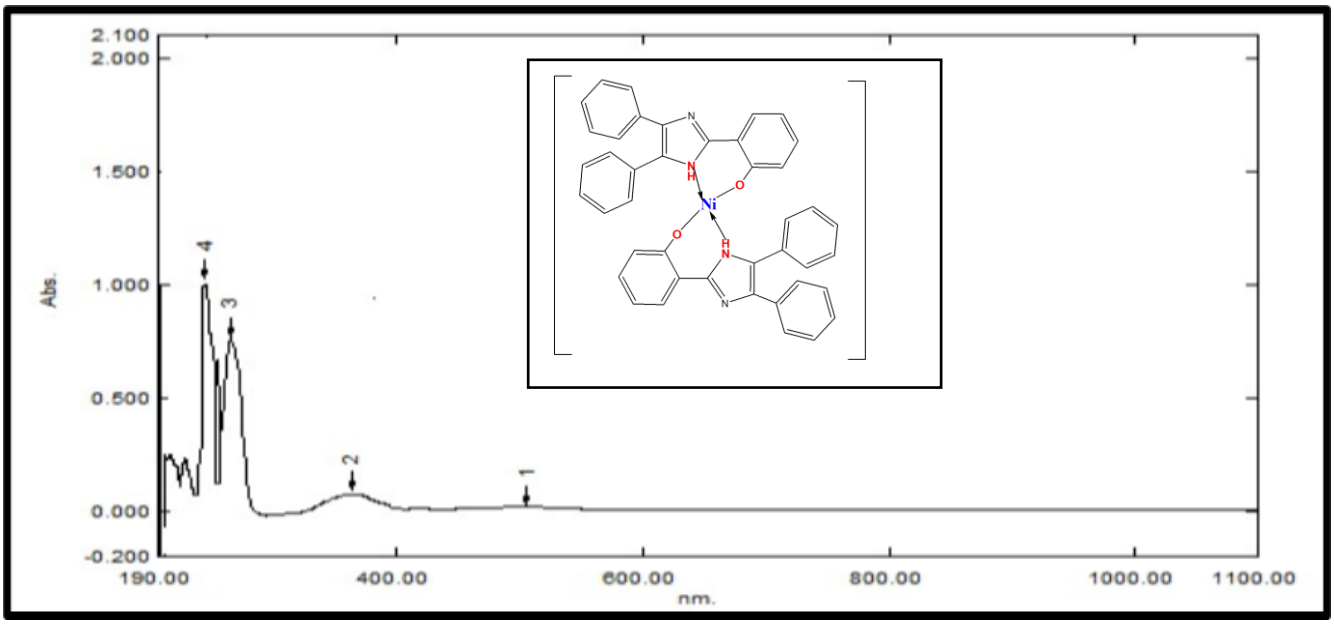

Fig. 7. Electronic spectrum of Ni(II)-L complex

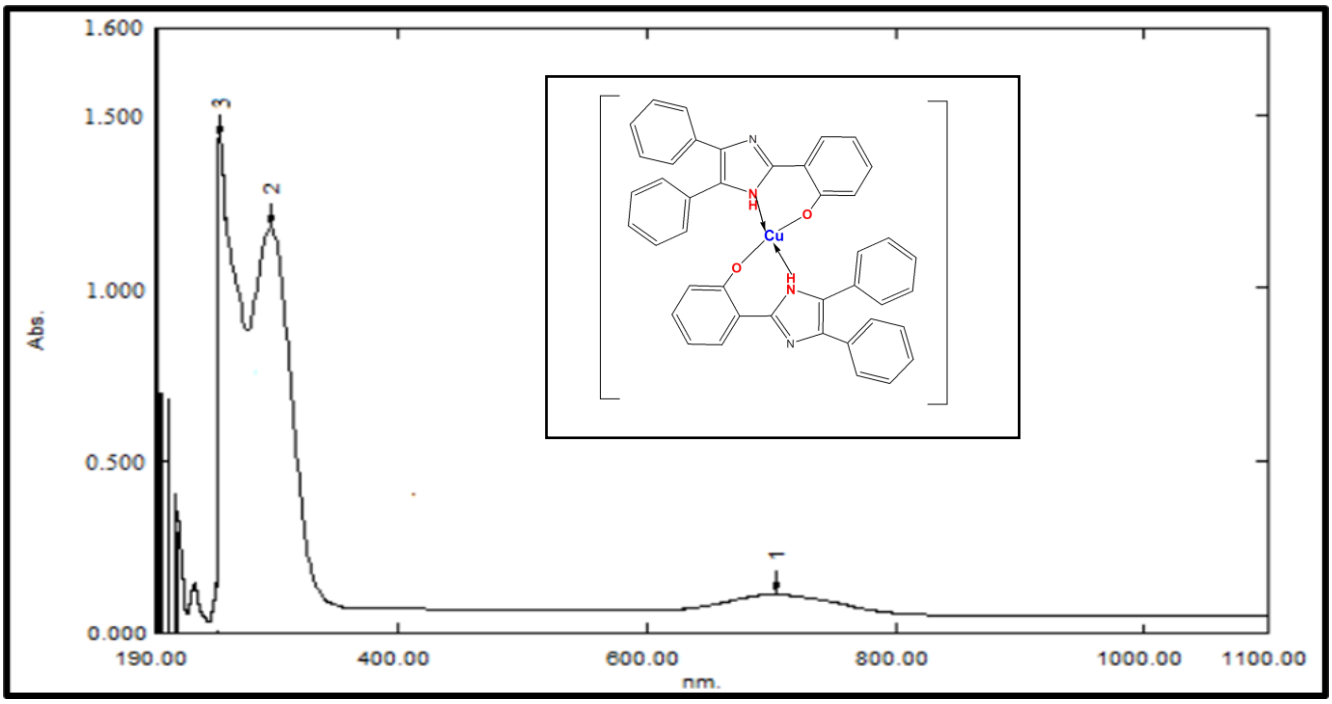

Fig. 8. Electronic spectrum of Cu(II)-L complex

IRAQI Academic Scientific Journals

AL ZAHRAA UNIVERSITY JOURNAL
Health and Medical Science

*Al-Zahraa Journal for Health and Medical Sciences 2026; 4(1):*215-242 **Vol. 4, No.1, 2026**
www.zjhms.alzahraa.edu.iq

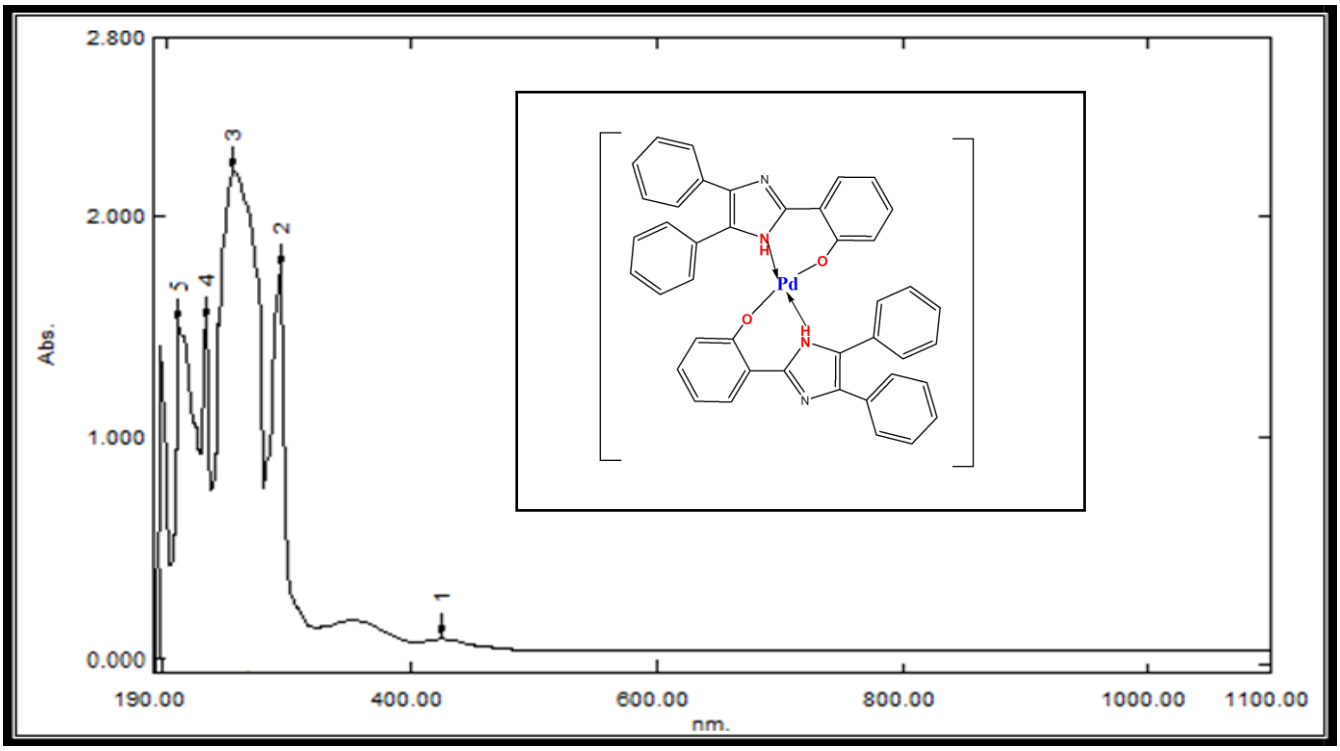

Fig. 9. Electronic spectrum of Pd(II)-L complex

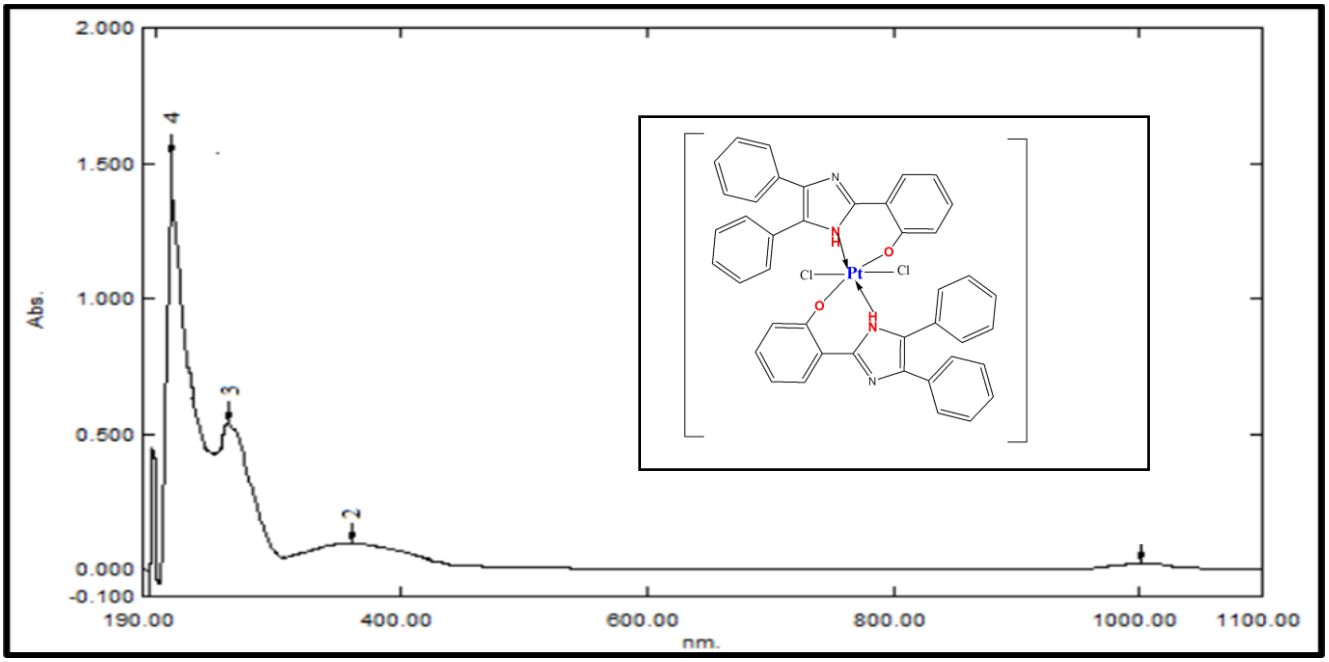

Fig. 10. Electronic spectrum of Pt(IV)-L complex

IRAQI Academic Scientific Journals

AL ZAHRAA UNIVERSITY JOURNAL
Health and Medical Science

*Al-Zahraa Journal for Health and Medical Sciences 2026; 4(1):*215-242 **Vol. 4, No.1, 2026**
www.zjhms.alzahraa.edu.iq

3.3. ^{1}H-NMR spectra of Ligand and complexes Ni and Pt

The 1H-NMR spectrum exhibited the following characteristic chemical shifts δ 12.5–13.0 ppm (s, 1H) attributed to the phenolic hydroxyl proton (O–H); (δ 8.50–8.20 ppm (weak to moderate signals, 1–2H) assigned to aromatic protons influenced by the electron-withdrawing effect of the imidazole nitrogen or other electron-withdrawing substituents; δ 8.00–7.60 ppm (m, several H) corresponding to aromatic protons of the phenyl rings; δ 7.50–7.10 ppm (broad m, majority of aromatic protons) representing overlapping benzene ring protons; and δ 7.80–7.00 ppm (s or weak d, 1H). The singlet observed at δ ≈ 12.5–13.0 ppm is assigned to the phenolic O–H proton. Its pronounced downfield position indicates strong intramolecular hydrogen bonding, most likely of the O–H···N(imidazole) type, resulting in significant deshielding of this proton [27]. Signals in the δ 8.2–8.5 ppm region are attributed to aromatic protons located in an electron-deficient environment due to the influence of the imidazole nitrogen atom or adjacent electron-withdrawing groups. The multiplet signals within δ 7.6–8.0 ppm correspond to part of the phenyl ring protons, where the observed splitting pattern arises from overlapping chemical shifts and similar coupling constants. The broad multiplet in the δ 7.1–7.5 ppm range accounts for the majority of the aromatic protons in the structure, reflecting the predominantly aromatic character of the ligand. Since the imidazole ring is tri-substituted, only one proton remains on the ring, appearing in the aromatic region at δ ≈ 7.0–7.8 ppm .Upon coordination to form the [Ni–L] and [Pt–L] complexes, a notable downfield shift is observed for the signals associated with protons near the coordination site [28]. This shift provides clear evidence of nitrogen–copper and nitrogen-platinum interaction and electron density withdrawal from the surrounding aromatic system. δ 6.8–8.2ppm this region exhibits multiple overlapping signals (multiplets) assigned to the imidazole ring protons (C4–H and C5–H). The relatively downfield chemical shifts are consistent with coordination of the imidazole nitrogen atom to the Cu^{2+} and Pt^{+4} center, resulting in electron density withdrawal from the ring and subsequent deshielding of these protons. While disappearance of the Phenolic Signal. The absence of the signal at δ 12.5–13.0 ppm in the complexes' spectra confirms the deprotonation of the hydroxyl group and the subsequent coordination of the phenolic oxygen to the metal center (Ni–O) and (Pt–O). δ ~2.5-3 ppm a strong resonance is attributed to the residual proton signal of the DMSO-d^{6} solvent and does not originate from the complex. The spectral data confirm the successful coordination of the ligand

IRAQI Academic Scientific Journals

AL ZAHRAA UNIVERSITY JOURNAL
Health and Medical Science

*Al-Zahraa Journal for Health and Medical Sciences 2026; 4(1):*215-242 **Vol. 4, No.1, 2026**
www.zjhms.alzahraa.edu.iq

to the metal centers via the oxygen (post-deprotonation) and nitrogen atoms. The observed deshielding patterns are consistent with strong metal-ligand interactions[29].

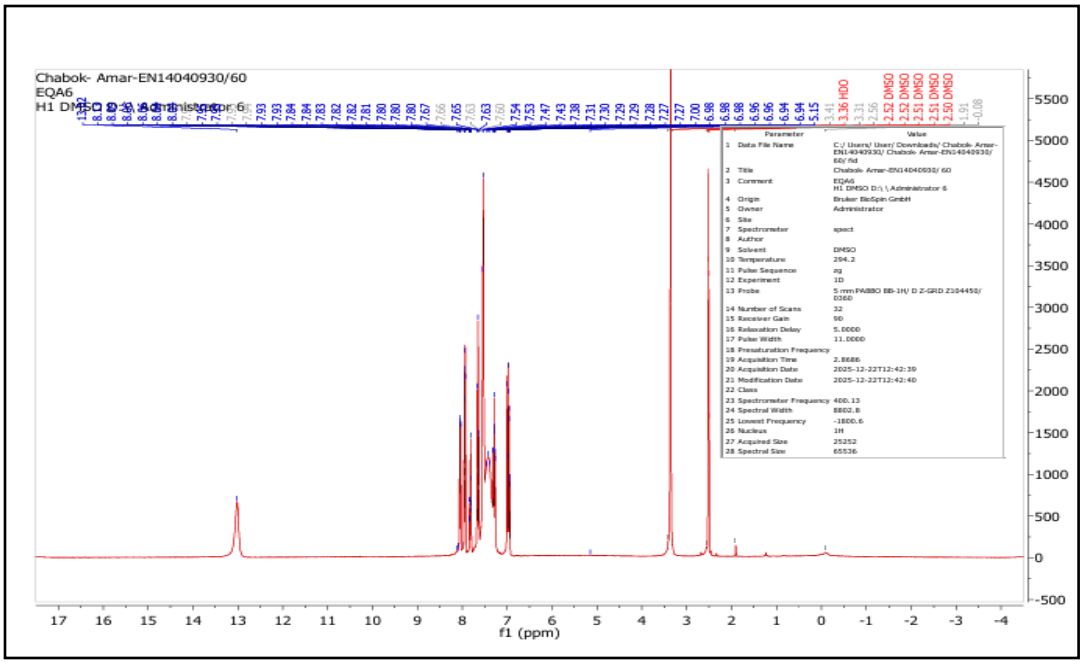

Fig. 11. 1H-NMR spectrum of ligand (L)

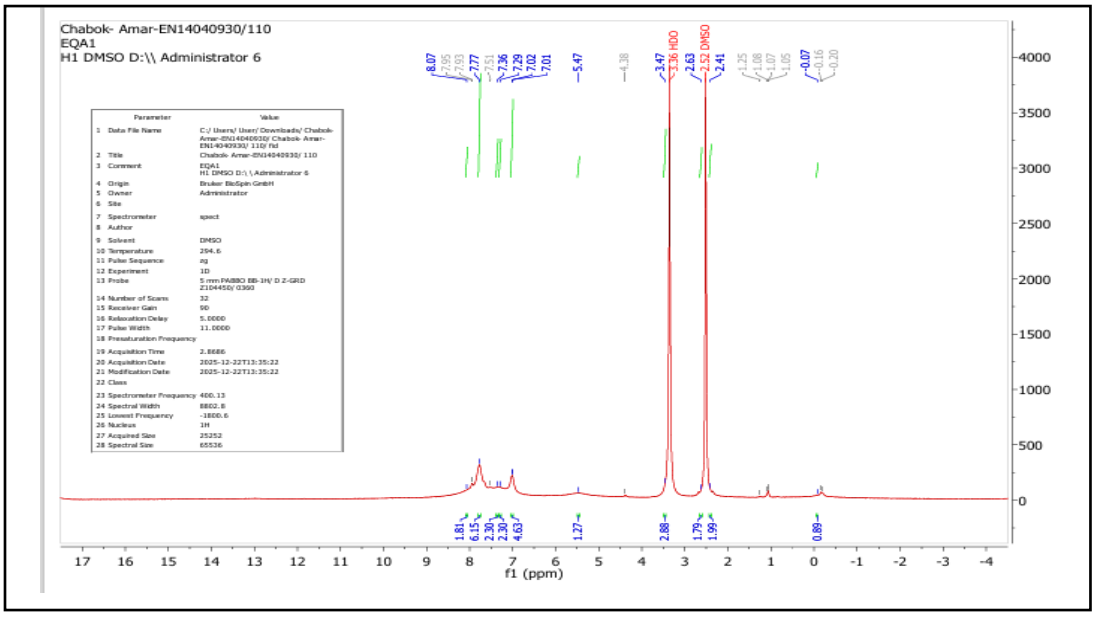

Fig. 12. 1H-NMR spectrum of Ni(II)-L complex

IRAQI Academic Scientific Journals

AL ZAHRAA UNIVERSITY JOURNAL
Health and Medical Science

*Al-Zahraa Journal for Health and Medical Sciences 2026; 4(1):*215-242 **Vol. 4, No.1, 2026**
www.zjhms.alzahraa.edu.iq

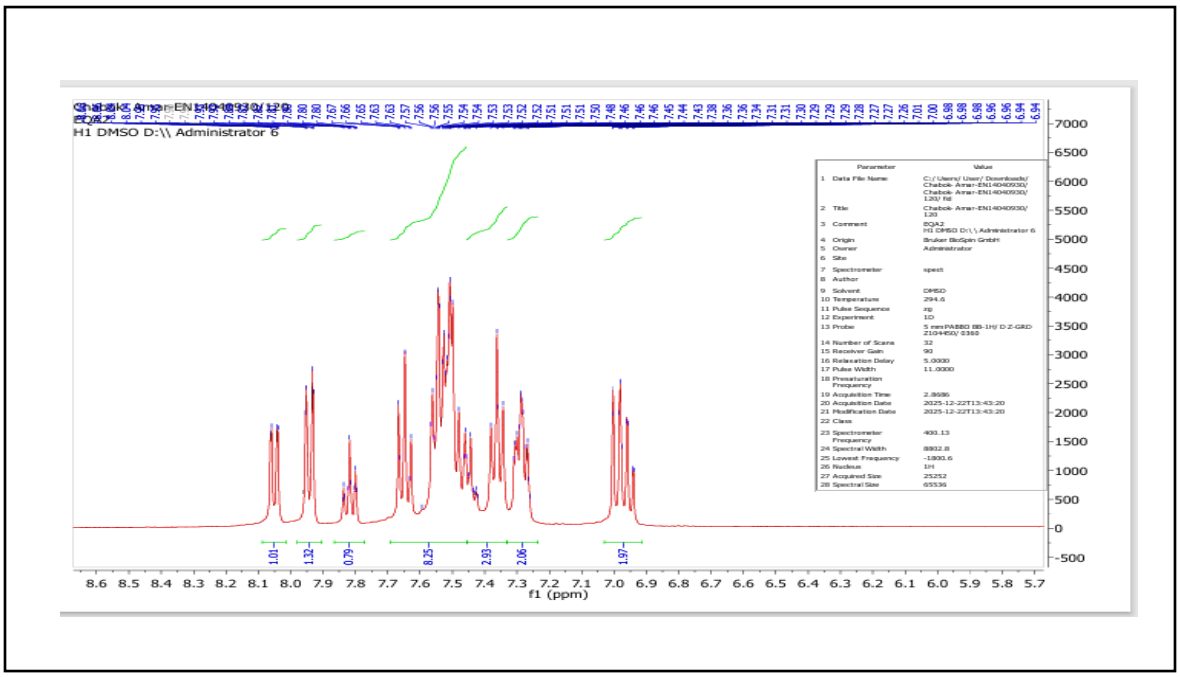

Fig. 13. 1H-NMR spectrum of Pt(IV)-L complex

3.4 Mass spectrum of the ligand(L)

The tri-substituted imidazole ligand with the molecular formula $C_{21}H_{16}N_2O$ was analyzed using direct mass spectrometry. The calculated molecular weight of the compound is 312.37 g/mol, which corresponds precisely to the observed molecular ion peak at m/z = 312.3 (M^{+}•). The high intensity of this peak reflects the considerable stability of the molecular ion, attributable to the aromatic nature of the compound, the presence of conjugated phenyl rings, and a delocalized π-system that enhances ion stabilization. A peak at m/z = 297 was observed, corresponding to the loss of a methyl group or a small fragment from a side chain, and can be assigned as $[M - 15]^{+}$.Another peak at m/z = 283 represents the $[M - 29]^{+}$ ion, indicative of the loss of a formyl group (CHO) or a small oxygen-containing fragment from the molecule. The peak at m/z = 165.1 is the base fragment and holds significant importance, typically representing an aromatic portion of the phenyl–imidazole system or a stabilized aromatic cation formed through cleavage of the molecule into two nearly equal fragments. The high stability of this ion is due to resonance and the aromatic character of the structure. The peak at m/z = 105 is commonly attributed to the benzoyl ion ($C_6H_5–CO^{+}$), a typical fragment observed in oxygen-containing aromatic

IRAQI Academic Scientific Journals

AL ZAHRAA UNIVERSITY JOURNAL
Health and Medical Science

*Al-Zahraa Journal for Health and Medical Sciences 2026; 4(1):*215-242 **Vol. 4, No.1, 2026**
www.zjhms.alzahraa.edu.iq

compounds. Finally, the peak at m/z = 77 corresponds to the phenyl cation ($C_6H_5^+$), a characteristic fragment commonly associated with benzene rings in mass spectra.

Table 4. Mass Spectrometry Fragmentation Data of the Ligand

m/z Value	Assigned Formula	Fragmentation Assignment	Fragment Type
312.3	$C_{21}H_{16}N_2O$	Molecular Ion peak (Parent Molecule)	$M^{+}\bullet$
297	$[C_{20}H_{13}N_2O]^+$	Loss of methyl group or rearrangement $[M - 15]^+$	Fragment
283	$[C_{20}H_{15}N_2]^+$	Loss of carbonyl/formyl group $[M - 29]^+$	Fragment
165.1	$[C_{13}H_9N_2]^+$	Fluorenyl-type cation or core imidazole cleavage	Intermediate
105	$[C_7H_5O]^+$	Benzoyl cation ($C_6H_5–CO^+$)	Fragment
77	$[C_6H_5]^+$	Phenyl cation (Loss of (C_6H_5 ring)	Fragment

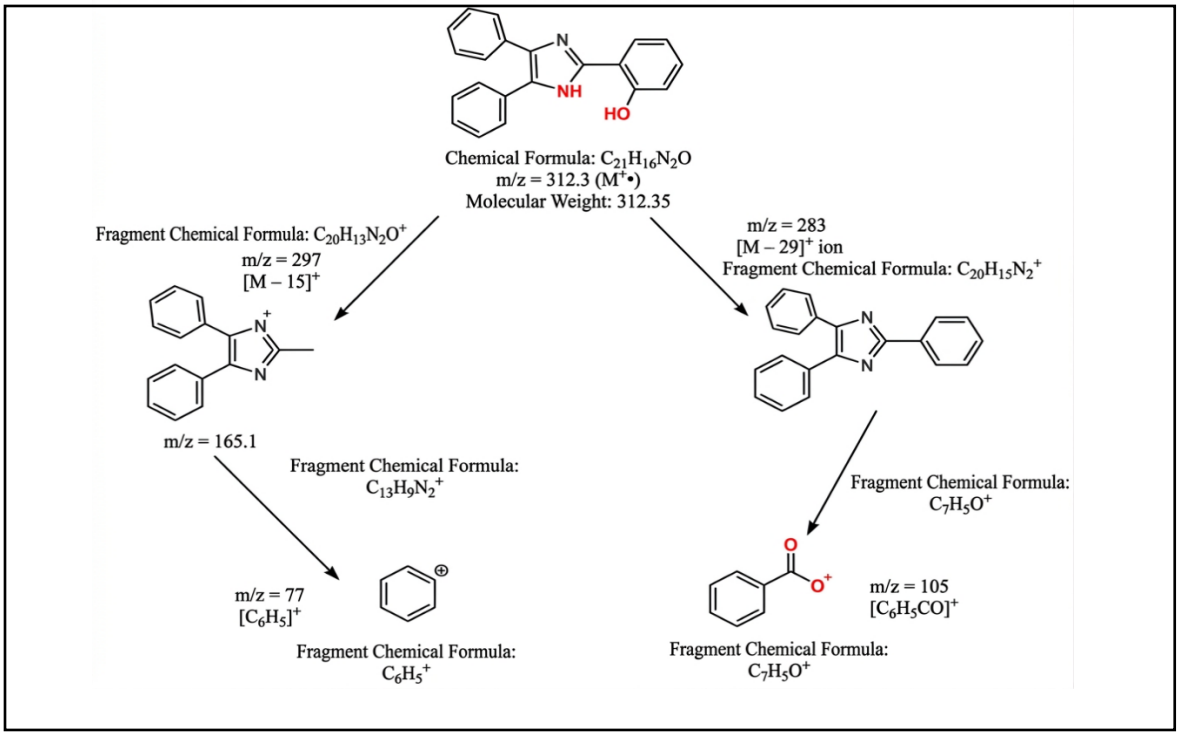

Fig. 14. Fragments ions in mass spectrum for ligand (L)

AL ZAHRAA UNIVERSITY JOURNAL
Health and Medical Science

*Al-Zahraa Journal for Health and Medical Sciences 2026; 4(1):*215-242 **Vol. 4, No.1, 2026**
www.zjhms.alzahraa.edu.iq

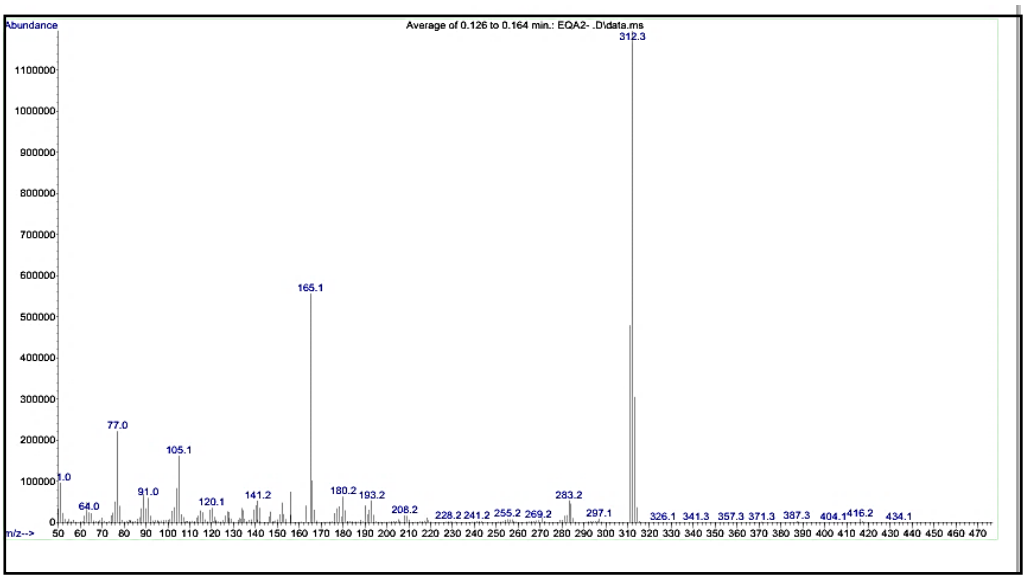

Fig. 15. Mass spectrum of the ligand (L)

4. Applications

4.1. Biological Activity

The antibacterial activity of the tri-imidazole ligand and its corresponding metal complexes (L-Ni, L-Cu, L-Pd, and L-Pt) was evaluated against two bacterial strains—one Gram-negative and one Gram-positive—as well as selected fungal species. The inhibition zone diameters recorded for the free ligand and its metal complexes are presented in Table 5. The results revealed that the majority of the tested compounds produced distinct zones of inhibition surrounding the impregnated disks, indicating significant antimicrobial activity. Notably, at higher concentrations, most of the metal complexes demonstrated superior antimicrobial efficacy compared to the free ligand, reflecting enhanced toxicity toward both bacterial and fungal strains. The synthesized ligand and its metal complexes exhibited greater inhibitory effects against Gram-positive bacteria, particularly *Streptococcus pneumoniae*, relative to the other examined microorganisms. The improved biological activity of these chelated complexes may be attributed to the involvement of metal ions in vital cellular functions. It is suggested that the incorporation of soft metal ions enhances the lipophilic character of the complexes, thereby promoting their diffusion across bacterial cell membranes and facilitating interactions within the intracellular environment [30].The pronounced antimicrobial effects observed for both the free

IRAQI Academic Scientific Journals

AL ZAHRAA UNIVERSITY JOURNAL
Health and Medical Science

*Al-Zahraa Journal for Health and Medical Sciences 2026; 4(1):*215-242 **Vol. 4, No.1, 2026**
www.zjhms.alzahraa.edu.iq

ligand and the newly synthesized mixed-metal complexes against *Streptococcus pneumoniae*, *Pseudomonas aeruginosa*, and *Candida albicans* can be rationalized based on Overtone's concept of cell permeability and Tweedy's chelation theory [31]. According to these principles, chelation reduces the polarity of the central metal ion through partial sharing of its positive charge with donor atoms of the ligand. This reduction in polarity enhances lipophilicity, thereby increasing membrane permeability and overall biological activity. Variations in the observed synergistic effects among different metal ions and their coordinated ligands may be attributed to several contributing factors, including the chelating capacity of the organic ligand, the nature and oxidation state of the central metal ion, the type of donor atoms involved in coordination, the coordination number, the spatial arrangement of ligands around the metal center, and the resulting geometric configuration of the complexes [14,20].Overall, the data presented in Table 5 and Figure (16) , demonstrate that both Gram-positive and Gram-negative bacterial strains, as well as the tested fungal species, exhibit sensitivity to the free ligand and the newly synthesized metal complexes.

Table 5. The ligand and its metal complex's antibacterial and antifungal activity, with an inhibitory zone measured in millimeters

Comp.	*Pseudomonas aeruginosa*			*Streptococcus pneumoniae*			*Candida albicans*		
Comp.	200	50	10	200	50	10	200	50	10
L	15	14	11	17	16	13	15	13	10
L-Ni	22	17	12	20	18	14	13	14	11
L-Cu	29	24	18	31	26	22	23	20	16
L-Pd	35	28	20	37	30	25	30	24	18
L-Pt	39	31	24	40	33	26	35	30	23

AL ZAHRAA UNIVERSITY JOURNAL
Health and Medical Science

*Al-Zahraa Journal for Health and Medical Sciences 2026; 4(1):*215-242 **Vol. 4, No.1, 2026**
www.zjhms.alzahraa.edu.iq

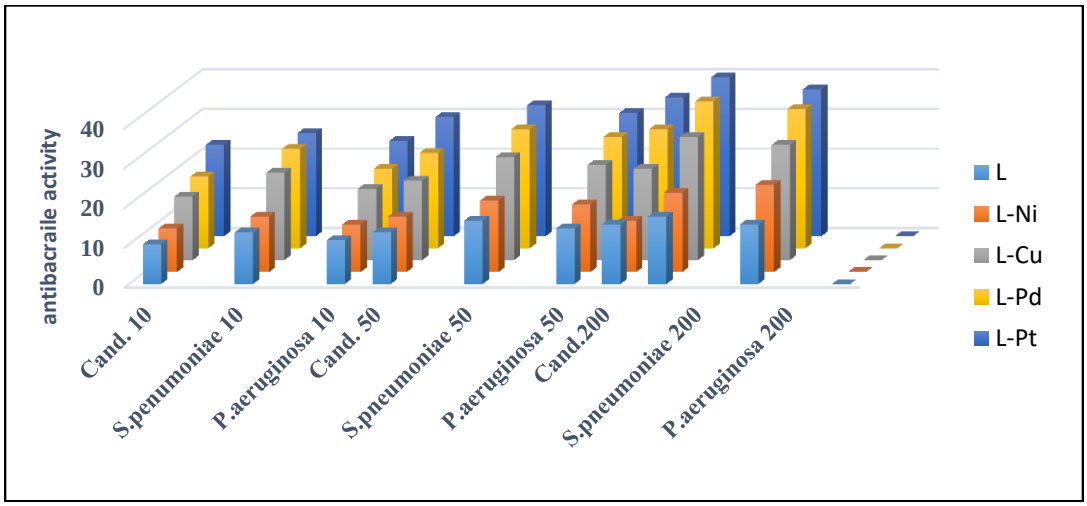

Fig. 16. Summary of anti-microbial activity of studying ligand and complexes

4.2. Anticancer of complexes

Breast cancer is the most common malignancy among women worldwide, accounting for approximately 25% of all female cancers, with particularly high incidence rates observed in numerous countries, including developed nations [32]. Subtypes of breast cancer are classified according to their histopathological characteristics as well as the expression profiles of hormone and growth factor receptors. Both genetic predisposition and non-genetic factors, such as environmental exposures and lifestyle, play significant roles in the initiation and progression of the disease. Radiotherapy remains a cornerstone in the management of breast cancer. Its cytotoxic effects arise either through direct damage to DNA or indirectly via the ionization of water molecules, which generates reactive species that induce macromolecular damage within cancer cells [33]. Despite the introduction of numerous novel chemotherapeutic agents, treatment outcomes are often suboptimal, highlighting the urgent need for the development of more effective anticancer compounds. Consequently, extensive research efforts are being directed toward the discovery and optimization of new pharmacological agents [34]. The present study evaluates the in vitro efficacy of synthetic ligands and their metal complexes against the human breast cancer cell line MDA-MB-231. Cytotoxicity and cell viability were assessed using the MTT assay following 24 hours of treatment with varying concentrations of the synthesized compounds. The results indicated that the metal complexes exhibited significantly higher

IRAQI Academic Scientific Journals

AL ZAHRAA UNIVERSITY JOURNAL
Health and Medical Science

*Al-Zahraa Journal for Health and Medical Sciences 2026; 4(1):*215-242 **Vol. 4, No.1, 2026**
www.zjhms.alzahraa.edu.iq

inhibitory activity compared to the free ligand. Notably, the synthesized platinum complex [L–Pt] demonstrated the highest potency among all the synthesis complexes. This enhancement in cytotoxicity is likely attributable to the specific geometrical configuration of the complexes, the oxidation state of the metal, and the inherent nature of the central metal ion, all of which contribute to improved biological efficacy. Furthermore, when compared to the clinical reference drug Cisplatin, the synthesized platinum complex exhibited superior activity, identifying it as a highly promising candidate for advanced metallotherapeutic application [35,36].

Table 6. Anticancer of ligand and complexes Inhibition µ/ mL

Com.	Conc. (µg/mL)					
	C 400	**C200**	**C100**	**C50**	**C25**	**C12.5**
L	**18%**	**15%**	**13%**	**10%**	**7%**	**4%**
L-Ni	**62%**	**58%**	**35%**	**29%**	**18%**	**16%**
L-Cu	**78%**	**71%**	**47%**	**36%**	**30%**	**25%**
L-Pd	**83%**	**78%**	**55%**	**48%**	**42%**	**38%**
L-Pt	**90%**	**82%**	**63%**	**57%**	**53%**	**41%**
Cisplatin	**85%**	**72%**	**55%**	**38%**	**24%**	**12%**

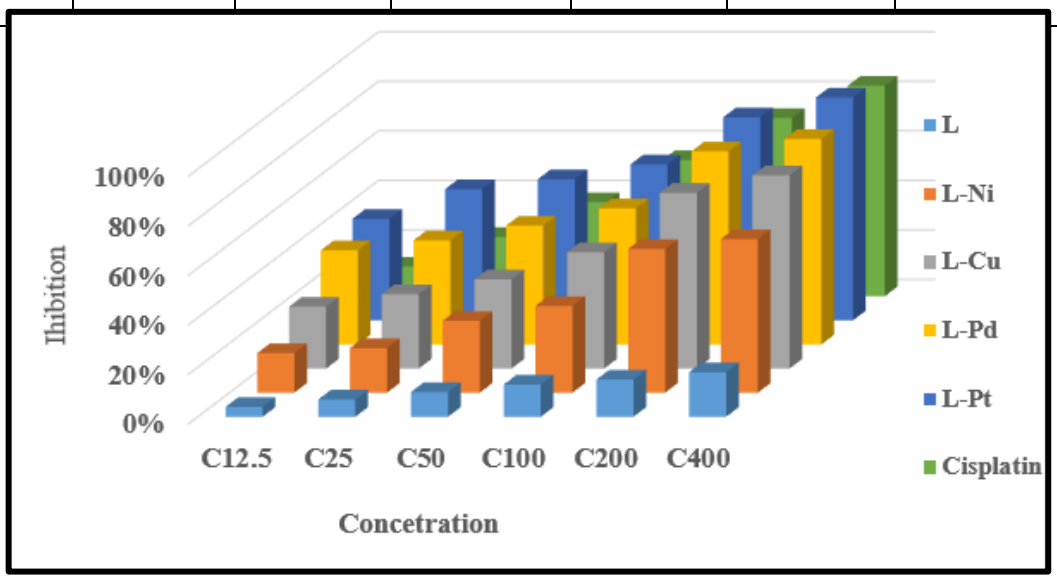

Fig. 17. Summary of anti-cancer activity of studying ligand and complexes.

IRAQI Academic Scientific Journals

AL ZAHRAA UNIVERSITY JOURNAL
Health and Medical Science

*Al-Zahraa Journal for Health and Medical Sciences 2026; 4(1):*215-242 **Vol. 4, No.1, 2026**
www.zjhms.alzahraa.edu.iq

Conclusions

This study investigated the synthesis of nickel, copper, palladium, and platinum metal complexes utilizing a tri-substituted imidazole derivative as the ligand. The complexes were prepared in a 1:2 molar ratio (metal:ligand), with the ligand functioning as a bidentate chelating agent through oxygen and nitrogen donor atoms. Structural characterization revealed that the palladium, nickel, and copper complexes adopted a square planer geometry, whereas the platinum complex exhibited an octahedral configuration. The synthesized ligand and complexes were further evaluated for their in vitro antimicrobial activity against both Gram-positive and Gram-negative bacteria, as well as *Candida albicans*. The results demonstrated that the biological activity of the compounds increased with concentration. Moreover, the metal complexes exhibited greater antimicrobial activity compared to the free ligand. Among the complexes tested, the platinum complex displayed the highest activity, which can be attributed to its specific geometrical configuration that enhances its biological performance. The synthesized complexes were evaluated for their anticancer activity against the MDA cell line. The results demonstrate a clear dose-dependent inhibitory effect, where the efficacy of the compounds against cancer cells increases proportionally with their concentration. Among the synthesized metal complexes, the Pt(IV) complex exhibited superior biological activity compared to the nickel, copper and palladium analogs. This enhanced potency is attributed to the synergistic impact of the platinum center, which likely facilitates more efficient interaction with biological targets, such as cellular DNA or enzyme active sites, leading to increased inhibition of cancer cell proliferation.

Acknowledgements

The authors sincerely thank all the staff who supported this manuscript in the College of Education and the Pure Science Department of Chemistry, University of Kerbala.

References

1. Abdulameer, J.H. and Mahasin F. Alias. (2022) ‘Heavy metal complexes of 1,2,3-triazole derivative: synthesis, characterization, and cytotoxicity appraisal against breast cancer cell lines (MDA-MB-231)’, Baghdad Science Journal, 19(6),pp.1410–1422. https://doi.org/10.21123/bsj.2022.7178

AL ZAHRAA UNIVERSITY JOURNAL
Health and Medical Science

*Al-Zahraa Journal for Health and Medical Sciences 2026; 4(1):*215-242 **Vol. 4, No.1, 2026**
www.zjhms.alzahraa.edu.iq

2. Zhu, X.-W., Luo, D., Zhou, X.-P. and Li, D. (2022) 'Imidazole-based metal-organic cages: synthesis, structures, and functions', Coordination Chemistry Reviews, 455, p.214354. https://doi.org/10.1016/j.ccr.2021.214354
3. Tolomeu, H.V. and Fraga, C.A.M. (2023) 'Imidazole: synthesis, functionalization and physicochemical properties of a privileged structure in medicinal chemistry', Molecules, 28(2), p.838. https://doi.org/10.3390/molecules28020838
4. El Azab, I.H., El-Sheshtawy, H.S., Bakr, R.B. and Elkanzi, N.A. (2021) 'New 1,2,3-triazole-containing hybrids as antitumor candidates: design, click reaction synthesis, DFT calculations, and molecular docking study', Molecules, 26(3), p.708. https://doi.org/10.3390/molecules26030708
5. Rani, P., Lal, K., Shrivastava, R. and Ghule, V.D. (2020) 'Synthesis and characterization of 1,2,3-triazoles-linked urea hybrid sensor for selective sensing of fluoride ion', Journal of Molecular Structure, 1203, p.127437. https://doi.org/10.1016/j.molstruc.2019.127437
6. El Azab, I.H., Elkanzi, N.A. and Gobouri, A.A. (2018) 'Design and synthesis of some new quinoxaline-based heterocycles', Journal of Heterocyclic Chemistry, 55(1), pp.65–76. https://doi.org/10.1002/jhet.2978
7. Riddell, I.A. and Lippard, S.J. (2018) 'Cisplatin and oxaliplatin: our current understanding of their actions', Metal Ions in Life Sciences, 18, pp.1–42. https://doi.org/10.1515/9783110470734-007
8. Kalash, K.R. and Al-Furaiji, M.H. (2020) 'Advanced oxidation of antibiotics polluted water using titanium dioxide in solar photocatalysis reactor', Journal of Engineering, 26(2), pp.1–13. https://doi.org/10.31026/j.eng.2020.02.01
9. Hassan, S.S., Hassan, N.M. and Baqer, S.R. (2021) 'Biological evaluation and theoretical study of bi-dentate ligand for amoxicillin derivative with some metal ions', Baghdad Science Journal, 18(4), p.1269. https://doi.org/10.21123/bsj.2021.18.4.1269
10. Abdulameer, J. and Mahasin F. Alias, M. (2022) 'Synthesis and characterization of some metal complexes with 2,6-bis(((1-octyl-1H-1,2,3-triazol-4-yl)methoxy)methyl)pyridine and the study of their biological activities', Eurasian Chemical Communications, 4, pp.1266–1284. DOI: 10.22034/ecc.2022.348852.1494

IRAQI Academic Scientific Journals

AL ZAHRAA UNIVERSITY JOURNAL
Health and Medical Science

*Al-Zahraa Journal for Health and Medical Sciences 2026; 4(1):*215-242 **Vol. 4, No.1, 2026**
www.zjhms.alzahraa.edu.iq

11. Fahmy, S.A., Preis, E., Bakowsky, U. and Azzazy, H.M.E.-S. (2020) 'Palladium nanoparticles fabricated by green chemistry: promising chemotherapeutic, antioxidant and antimicrobial agents', Materials, 13(17), p.3661. https://doi.org/10.3390/ma13173661
12. Brahim, A.A., Kareem, M.M., Al-Noor, T.H., Al-Muhimeed, T., AlObaid, A.A., Albukhaty, S., Sulaiman, G.M., Jabir, M., Taqi, Z.J. and Sahib, U.I., (2021) 'Pt(II)-thiocarbohydrazone complex as cytotoxic agent and apoptosis inducer in Caov-3 and HT-29 cells through the P53 and caspase-8 pathways', Pharmaceuticals, 14(6), p.509. https://doi.org/10.3390/ph14060509
13. Demehin, A.I., Oladipo, M.A. and Semire, B. (2019) 'Synthesis, spectroscopic, antibacterial and antioxidant activities of Pd(II) mixed-ligand complexes containing tridentate Schiff bases', Egyptian Journal of Chemistry, 62(Special Issue, Part 2: Innovation in Chemistry), pp.413–426. DOI: 10.21608/ejchem.2019.12319.1766
14. Abdulameer, J.H., Adnan I. M., Mahasin F. A., and Muntahaa A. R., (2026) 'Theoretical and Experimental Study Using Hyperchem-8 and Gaussian Computer Program to Study the Stability, Binding Energies, and Electrical Characteristics of Triazole-Based Metal Complexes in the Gas Phase', Engineering Chemistry, 13, pp.23–38. https://doi:10.4028/p-9tPQ07.
15. Ibrahim,A.A.MohanadM.Kareem,TaghreedH.Al-Noor, Tahani Al-Muhimeed,Tahani Al-Muhimeed, Abeer A. AlObaid, Salim Albukhaty, Ghassan M. Sulaiman, Majid Jabir, Zainab J.Taqi and UsamaI.(2021)'Pt(II)-thiocarbohydrazone complex as cytotoxic agent and apoptosis inducer in Caov-3 and HT-29 cells through the P53 and caspase-8 pathways', Pharmaceuticals, 14(6), p.509. https://doi.org/10.1016/j.bioelechem.2021.107936
16. Hrioua, A., A. Loudiki A. Farahi, F. Laghrib , M. Bakasse, S. Lahrich, S. Saqrane a, M.A. El Mhammedi. (2021) 'Complexation of amoxicillin by transition metals: physico-chemical and antibacterial activity evaluation', Bioelectrochemistry, 142, p.107936. https://doi.org/10.1016/j.bioelechem.2021.107936
17. Jawad, S.A.-A. and Kareem, I.K. (2022) 'Synthesis, characterization and biological study of open multi dentate new azo-Schiff ligand and its divalent metal ion complexes with copper, zinc and mercury', in AIP Conference Proceedings, 2386(1), AIP Publishing. https://doi.org/10.1063/5.0066818

AL ZAHRAA UNIVERSITY JOURNAL
Health and Medical Science

*Al-Zahraa Journal for Health and Medical Sciences 2026; 4(1):*215-242 **Vol. 4, No.1, 2026**
www.zjhms.alzahraa.edu.iq

18. Karem, L.K.A. and Al-Noor, T.H. (2020) 'Mixed ligand complexes of Schiff base and nicotinamide: synthesis, characterization and antimicrobial activities', in Journal of Physics: Conference Series, 1660(1), p.012094, IOP Publishing. DOI 10.1088/1742-6596/1660/1/012094
19. El-Betany, A. (2010) Synthesis and study of fluorescent dendritic molecules. PhD thesis, Cardiff University, United Kingdom.
20. Abdulameer, J.H. and Mahasin F. Alias, M.F. (2022) 'Synthesis, characterization and antimicrobial activity of Cu(II), Pt(IV) and Au(III) complexes with 2,6-bis(((1-decyl-1H-1,2,3-triazole-4-yl)methoxy)methyl)pyridine'.
21. Gülfen, M., Canbaz, Y. and Özdemir, A. (2020) 'Simultaneous determination of amoxicillin, lansoprazole, and levofloxacin in pharmaceuticals by HPLC with UV–Vis detector', Journal of Analysis and Testing, 4, pp.45–53.
22. Mohamad, H.A., Al-Kattan, W.T., Al-Daly, Z.M. and Najim, A.N. (2020) 'Synthesis, characterization and cytotoxicity of Ni(II), Pd(II), Pt(II) complexes with 6-methoxy-2,3,4,5-tetrahydropyridine (MTP)', Oriental Journal of Chemistry, 36(5), p.903. http://dx.doi.org/10.13005/ojc/360515
23. Al-Hamdani, A.A.S. and Hamoodah, R.G. (2016) 'Transition metal complexes with tridentate ligand: preparation, spectroscopic characterization, thermal analysis and structural studies',Baghdad Science Journal, 13(4), p.770. https://doi.org/10.21123/bsj.2016.13.4.0770
24. Alibrahim, K., Al-Saif, F., Bakhsh, H. and Refat, M. (2018) 'Synthesis, physicochemical, and biological studies of new pyridoxine HCl mononuclear drug complexes of V(III), Ru(III), Pt(II), Se(IV), and Au(III) metal ions', Russian Journal of General Chemistry, 88,pp. 2400–2409.
25. Ahmed S. Faihan , Mohammad R. Hatshan, Mustafa M. Kadhim, Ali S. Alqahtani, Fahd A. Nasr , Abdulrahman M. Saleh, Subhi A. Al-Jibori, Ahmed S. Al-Janabi . (2022) 'Promising bio-active complexes of platinum (II) and palladium (II) derived from heterocyclic thiourea: synthesis, characterization, DFT, molecular docking, and anti-cancer studies', Journal of Molecular Structure, 1252, p.132198. https://doi.org/10.1016/j.molstruc.2021.132198
26. El-Sonbati, A., N.F. Omar , M.I. Abou-Dobara b, M.A. Diab, M.A. El-Mogazy , Sh.M. Morgan, M.A. Hussien, A.A. El-Ghettany. (2021) 'Structural, molecular docking computational studies and in-vitro evidence for antibacterial activity of mixed ligand

complexes',Journal of Molecular Structure, 1239, p.130481. https://doi.org/10.1016/j.molstruc.2021.130481

27. Khan, S.A., Ullah, Q., Parveen, H., Mukhtar, S., Alzahrani, K.A. and Asad, M. (2021) 'Synthesis and photophysical investigation of novel imidazole derivative an efficient multimodal chemosensor for Cu(II) and fluoride ions', Journal of Photochemistry and PhotobiologyA:Chemistry,406, p.113022. https://doi.org/10.1016/j.jphotochem.2020.113022
28. Thakar, M.A., Jha, S.S., Phasinam, K., Manne, R., Qureshi, Y. and Babu, V.H. (2022) 'X ray diffraction (XRD) analysis and evaluation of antioxidant activity of copper oxide nanoparticles synthesized from leaf extract of Cissus vitiginea', Materials Today: Proceedings, 51,pp. 319–324. https://doi.org/10.1016/j.matpr.2021.05.410
29. Zahraa M. Shaker; Hamida Idan Salman; and Mohammad N. AL-Baiati. (2023) 'Removal of reactive yellow 145 dye pollutant from wastewater by using a nano surface', in AIP Conference Proceedings, 2414(1), AIP Publishing. https://doi.org/10.1063/5.0114870
30. Abouzayed, F.I., Emam, S.M. and Abouel-Enein, S.A. (2020) 'Synthesis, characterization and biological activity of nano-sized Co(II), Ni(II), Cu(II), Pd(II) and Ru(III) complexes of tetradentate hydrazone ligand', Journal of Molecular Structure, 1216, p.128314. https://doi.org/10.1016/j.molstruc.2020.128314
31. Kalimuthu, K., Cha, B.S., Kim, S. and Park, K.S. (2020) 'Eco-friendly synthesis and biomedical applications of gold nanoparticles: a review', Microchemical Journal, 152, p.104296. https://doi.org/10.1016/j.microc.2019.104296
32. Sharmin, S., Md. Mizanur Rahaman, Miquel Martorell, Jorge Sastre-Serra, Javad Sharifi-Rad, Monica Butnariu, Iulia Cristina Bagiu, Radu Vasile Bagiu & Mohammad Torequl Islam. (2021) 'Cytotoxicity of synthetic derivatives against breast cancer and multi-drug resistant breast cancer cell lines: a literature-based perspective study', Cancer Cell International, 21, pp.1–19
33. Ma, S., Xinxin Fu ,Lin Liu, Yi Liu ,Hao Feng ,Heya Jiang ,Xiaomei Liu ,Rui Liu, Zhenzhen Liang , Mengke Li ,Zhujun Tian ,Boqi Hu ,Yongheng Bai ,Bing Liang ,Xiaodong Liu. (2021) 'Iron-dependent autophagic cell death induced by radiation in MDA-MB-231 breast cancer cells', Frontiers in Cell and Developmental Biology, 9, p.723801. https://doi.org/10.3389/fcell.2021.723801

AL ZAHRAA UNIVERSITY JOURNAL
Health and Medical Science

*Al-Zahraa Journal for Health and Medical Sciences 2026; 4(1):*215-242 **Vol. 4, No.1, 2026**
www.zjhms.alzahraa.edu.iq

34. Ali, F.J., Radhi, I.J., Salman, H.I. and Hassan, S.A. (2025). Study the efficiency of cement kiln dust waste for removal of some dyes. Chemical Review and Letters, 8(1), pp.187-198. https://doi.org/10.22034/crl.2025.479727.1443
35. Ando, T. (2021) 'Biophysical reviews top five: atomic force microscopy in biophysics', Biophysical Reviews, 13,pp. 455–458. https://doi.org/10.1007/s12551-021-00820-x.
36. Hussein, S.S., Al Hindawi, A.M. and Abdulameer, J.H. (2025) 'A theoretical investigation of the electronic and molecular properties of Zn_3Se_3-EDTA in nanostructures using DFT methodology', in AIP Conference Proceedings. AIP Publishing LLC, 50016. https://doi.org/10.1063/5.0303010.

IRAQI Academic Scientific Journals